

# Shear-Induced Clustering in a Simple Driven Diffusive Model

O.J. O'Loan, M.R. Evans and M.E. Cates

*Department of Physics and Astronomy, University of Edinburgh, Mayfield Road, Edinburgh EH9 3JZ, U.K.*

---

## Abstract

We study a simple lattice model of shear-induced clustering in two dimensions in which clusters of particles aggregate under an imposed shear flow and fragment stochastically. Two non-equilibrium steady states are identified: an unjammed state and a jammed state characterised by a system-spanning cluster. A discontinuous jamming transition with strong hysteresis occurs as the shear rate is increased or fragmentation rate decreased. We study the kinetics of jamming and measure power law cluster size distributions. We also consider some general simulation issues including the role of Galilean invariance.

---

## 1 Introduction

When subjected to shear flow, many complex fluids exhibit shear thickening behaviour where viscosity increases with shear rate. Shear thickening is often discontinuous and may be accompanied by hysteresis and structural changes. Systems where such behaviour has been observed include concentrated colloidal suspensions [1] and rodlike micelle solutions [2].

In the case of colloidal suspensions, it has been suggested that shear thickening is the result of the formation of hydrodynamic clusters [3]. These clusters comprise large numbers of particles bound together by short-range lubrication forces and form along the compression axis of the shear. Indeed a detailed analysis of the dynamics of the aggregation of such rotating clusters, in the absence of Brownian motion, has recently been performed [4] and suggests that the discontinuous jump in viscosity is due to a jamming transition where, essentially, a log-jam of clusters occurs.

Jamming transitions have also been studied in an apparently different context, that of driven diffusive systems [5]. In one dimensional models, jams have

been induced by the presence of defects or disorder [6] or by a non-conserved quantity mediating an effective long-range interaction [7]. In two-dimensional ( $2d$ ) driven lattice gases, gridlock effects have been studied [8,9].

Recently, Santra and Herrmann introduced a simple  $2d$  lattice model of gelation under shear [10], which provides a link between colloidal systems and driven lattice gases. They showed that within the model one finds dynamical scaling as clusters of particles aggregate irreversibly, and that the clusters are aligned roughly along the compression axis of the shear. The model has been extended to take into account the effect of rotation of the clusters [11].

In the present work, we extend the model of [10] in a different direction by allowing clusters to fragment stochastically. This models thermal fluctuations in a simple manner and gives rise to the possibility of non-trivial steady states, in contrast to the absorbing state consisting of a single cluster which is always attained with the models of [10] and [11]. Indeed, as we shall show below, we find two types of steady state – *unjammed*, where clusters have some typical size much smaller than the transverse size of the system, and *jammed*, in which there are clusters which span the system. We provide evidence of a discontinuous transition between the two states, with hysteresis, as the fragmentation rate or the shear rate is varied. We study the kinetics of the jamming process and find evidence for dynamical scaling for both zero and non-zero fragmentation rate. Although there is an intriguing similarity with the colloidal jamming problem studied in [4], in practice the transitions we observe arise at very low concentration. In this respect the behaviour is more like that of the micellar problem of [2].

The paper is organised as follows. In section 2 we define the model that we study and simulation results are presented in section 3. In section 4 more general issues concerning the simulations are raised. We conclude in section 5.

## 2 Description of the Model

The model is defined on a  $2d$  lattice of length  $L$  and width  $W$ , illustrated by an example configuration in figure 1. Each lattice site is either occupied by a particle or empty. The boundary perpendicular to the direction of flow is periodic but no particles may pass through the boundaries parallel to the direction of flow – they are “hard walls”. A simple shear flow is imposed by assigning a velocity  $v(y)$  to each “lane” in the direction of flow given by

$$v(y) = v(0) + \dot{\gamma}y \quad (1)$$

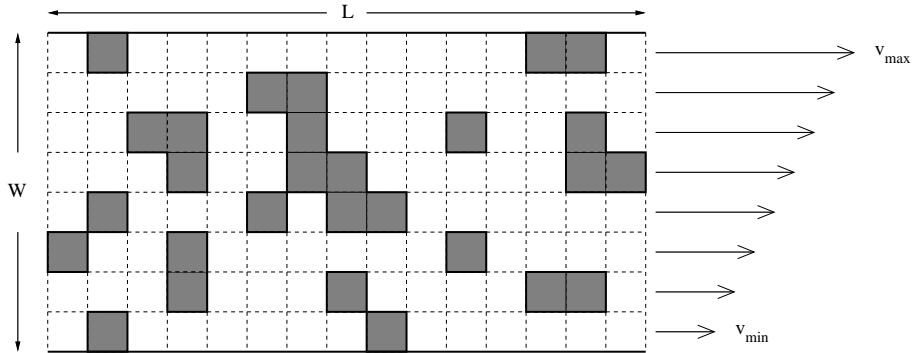


Fig. 1. Example lattice configuration. The shear flow is represented by the arrows.

where  $y$  runs from 0 to  $W - 1$ . Each particle in lane  $y$  is said to have velocity  $v(y)$ . Hence, the shear rate is

$$\dot{\gamma} = \frac{v_{\max} - v_{\min}}{W - 1} \quad (2)$$

where  $v_{\min} = v(0)$  and  $v_{\max} = v(W - 1)$ . We consider only non-negative velocities from now on. There are  $N$  particles in the system and the concentration is

$$c = \frac{N}{WL}. \quad (3)$$

We define a cluster to be a set of particles connected successively by nearest-neighbour bonds on the lattice. Therefore, the nearest neighbour sites belonging to an individual particle are either empty or occupied by particles in the same cluster. The velocity  $u$  of a cluster is defined as the mean of the velocities of its constituent particles. The proximity of a wall does not affect the velocity of a cluster so that one may think of the particles “slipping” relative to the walls. (In contrast, in order to set up a shear flow in a fluid by moving one or both of the walls, a no-slip condition between the *fluid* and the walls is required.)

A (continuous) “counter” variable  $q$  is associated with each cluster. In each simulation time-step, three steps (flow, cluster merging and fragmentation) are performed in the following sequence:

**Flow** The counter  $q$  for each cluster is incremented by  $u$ , the cluster velocity.

If  $q \geq 1$  for any cluster, all the particles in that cluster move one site forward (*i.e.* in the direction of flow) and  $q \rightarrow q - 1$ . If  $q < 1$ , no action is taken.

**Cluster merging** At the end of the previous step, some clusters may have become connected and these clusters are now merged. In merging two clus-

ters, the resulting single cluster is assigned a counter which is the weighted average of the counters of the two constituent clusters labelled  $i$  and  $j$ :

$$q_{i+j} = \frac{n_i q_i + n_j q_j}{n_i + n_j} \quad (4)$$

where  $n_i$  is the number of particles in cluster  $i$ . We have checked that this ensures that the average velocity of clusters in lane  $y$  is indeed  $v(y)$ .

**Fragmentation** This random sequential step allows single particles to leave clusters, possibly resulting in the break up of clusters. The following update rules are repeated  $N$  times:

- (1) A particle is chosen at random.
- (2) A direction for the particle to move is chosen at random from the four possibilities.
- (3) If the particle is not blocked by another particle in the chosen direction, it moves one site in that direction with probability  $T$ , where  $T$  may be thought of as the “temperature” of the system.
- (4) The moved particle becomes a single-particle cluster with counter variable equal to that of the cluster it previously belonged to. If it adjoins any other clusters, this single-particle cluster is then merged as detailed previously.

The fragmentation update of one particle may result in one of five outcomes: no change, a particle leaving its cluster, a particle moving to a different location in the same cluster, movement of a single-particle cluster or a single-particle cluster joining another cluster.

The three physical parameters present in the model are concentration  $c$ , shear rate  $\dot{\gamma}$  and “temperature”  $T$ .

Simple shear flow is Galilean invariant, by which we mean that adding a constant velocity at every point in the system has no effect on the physics. It is therefore desirable that any model of simple shear is as close as possible to being Galilean invariant. We discuss this issue in section 4 where we show that lattice effects break Galilean invariance in the model. In addition, we remark that the model is translationally invariant only in the direction of flow. The fixed walls break translational invariance normal to the direction of flow.

### 3 Results

#### 3.1 Steady State Behaviour

From computer simulation of the model defined in section 2, we have found two types of steady state. The first is an unjammed state, where many small

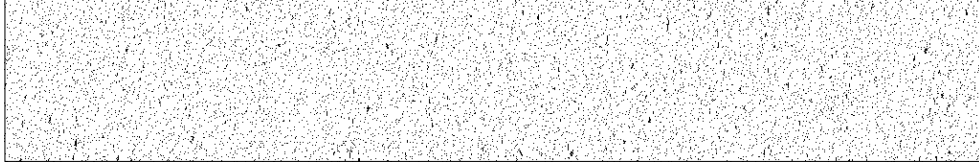


Fig. 2. Snapshot of an unjammed  $1200 \times 200$  system in the steady state. The simulation parameters were  $c = 0.07$ ,  $T = 0.0045$  and  $\dot{\gamma} = 5/1990 \simeq 0.0025$ . The flow is from left to right and the velocity increases from bottom to top.

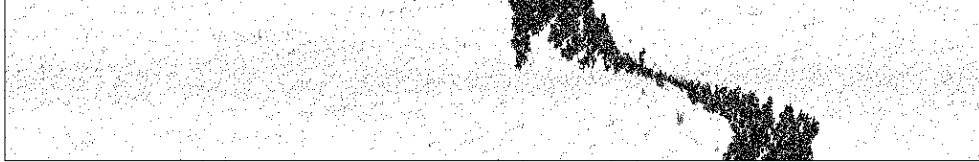


Fig. 3. Snapshot of a jammed  $1200 \times 200$  system in the steady state. The simulation parameters were the same as for figure 2 with the exception that here  $\dot{\gamma} = 7/1990 \simeq 0.0035$ .

clusters are evenly distributed throughout the system. A snapshot of a typical unjammed system is shown in figure 2. There are some clusters which are elongated perpendicular to the direction of flow but the typical cluster size is very small.

A second type of steady state exhibited by the model is characterised by the presence of clusters which span the system; we refer to it as “jammed” state (although the spanning cluster is not stationary). These *spanning clusters* contain a finite fraction of the particles in the system. A snapshot of a typical jammed system is shown in figure 3; the system is strongly inhomogeneous in a number of respects. Since the spanning cluster is moving with a velocity close to that of the particles in the centre of the channel, the rate of aggregation is least in the centre and greatest at the walls – near the upper wall, small clusters move more quickly than the spanning cluster and join it from behind whereas near the lower wall, small clusters move more slowly than the spanning cluster and aggregate from the front. Hence the spanning cluster is aligned at an angle to the direction of flow and decreases in thickness from the edges to the centre of the channel. Accordingly, the density in the rest of the system is greatest in the centre and least at the edges. Some quite large clusters are visible close to the spanning cluster – these are probably pieces of the spanning cluster which broke off some short time previously. The somewhat unusual, inhomogeneous nature of the jammed steady state in the finite systems we study is primarily a result of having hard wall boundaries parallel to the direction of flow rather than any effect of the underlying square lattice.

In order to discuss the behaviour of the model more quantitatively, we introduce the cluster size distribution  $n(m, t)$ , the number of clusters containing  $m$  particles at time  $t$ . The moments  $M_k(t)$  of the cluster size distribution are

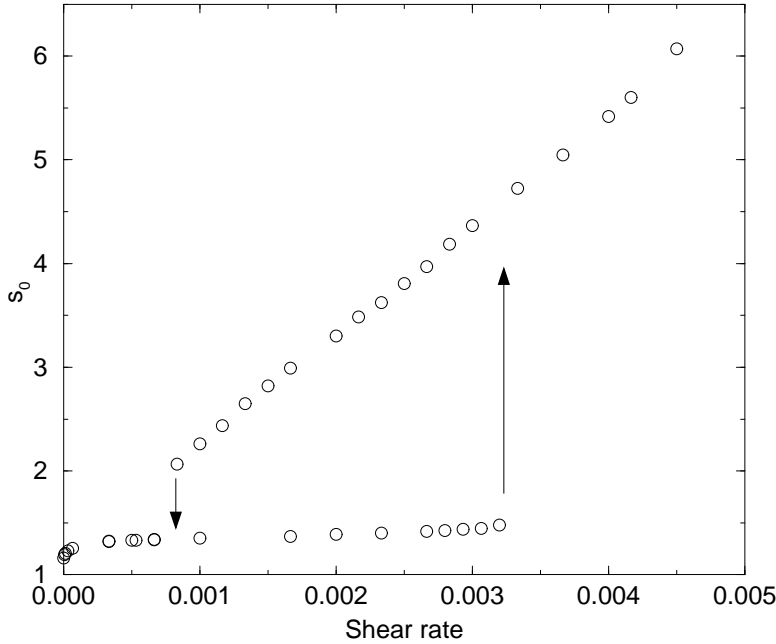


Fig. 4. Plot of  $s_0$  against  $\dot{\gamma}$  for a  $900 \times 150$  system with  $c = 0.07$  and  $T = 0.0045$ . The direction of the hysteresis loop is shown by the arrows.

given by

$$M_k(t) = \sum_{m=1}^{\infty} m^k n(m, t) \quad (5)$$

so that  $M_1 = N$ , the number of particles in the system and  $M_0$  is the number of clusters in the system. We define

$$s_k(t) = \frac{M_{k+1}(t)}{M_k(t)} \quad (6)$$

as measures of typical cluster size [12] for  $k \geq 0$ . In discussing steady state properties of the system, we use the average cluster size  $s_0$  as our measure of typical cluster size since this quantity is not dominated by the spanning clusters in jammed systems. In contrast, for  $k > 0$ ,  $s_k$  is of the order of the size of a spanning cluster in the jammed state. We use  $s_1$  when discussing the kinetics of jamming in section 3.2.

We now provide evidence of a strong discontinuous phase transition between jammed and unjammed states as the parameters  $T$  and  $\dot{\gamma}$  are varied. Figure 4 shows a plot of  $s_0$  against  $\dot{\gamma}$ . Strong hysteresis is apparent, with the direction of the hysteresis loop shown by the arrows. As  $\dot{\gamma}$  is increased from zero,

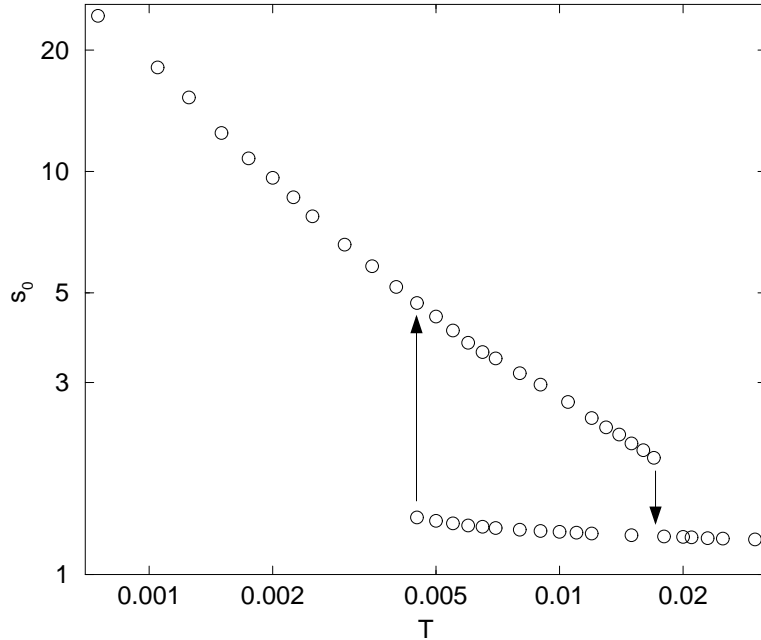


Fig. 5. Log-log plot of  $s_0$  against  $T$  for a  $900 \times 150$  system with  $c = 0.06$  and  $\dot{\gamma} = 6/1490 \simeq 0.004$ . The direction of the hysteresis loop is shown by the arrows.

$s_0$  increases smoothly at first but jumps discontinuously to a larger value, corresponding to a jammed system. When  $\dot{\gamma}$  is then decreased, the jammed state remains stable (for at least  $2 \times 10^5$  time-steps) for a range of  $\dot{\gamma}$  values in which an unjammed state is also stable (for at least  $10^5$  time-steps). The system becomes unjammed again for sufficiently small  $\dot{\gamma}$  (*i.e.* an initially jammed configuration becomes unstable). One can also see from figure 4 that, for jammed systems,  $s_0$  increases roughly linearly with increasing shear rate.

Similar behaviour is found when  $T$  is varied with  $\dot{\gamma}$  and  $c$  held fixed. Figure 5 shows a log-log plot of  $s_0$  against  $T$ . As in figure 4, strong hysteresis is apparent. There is a large range of values of  $T$  for which both unjammed and jammed states are stable (on a time-scale of at least  $2 \times 10^5$  time-steps for jammed systems and at least  $10^5$  time-steps for unjammed systems.)

Figure 6 shows a log-log plot of the steady state cluster size distribution  $n(m)$  for both unjammed and jammed systems at the same value of  $T = 0.006$ . In the homogenous system,  $n(m)$  decays very rapidly and the large  $m$  behaviour appears to be exponential (it decays faster than any power law). In the jammed system, the size distribution of small (non-spanning) clusters only is shown; the distribution as a whole is bimodal, with the second peak (not shown) corresponding to the spanning cluster. The figure suggests that for the small clusters,  $n(m)$  decays as a power of  $m$  (for  $m$  greater than about 10) with an

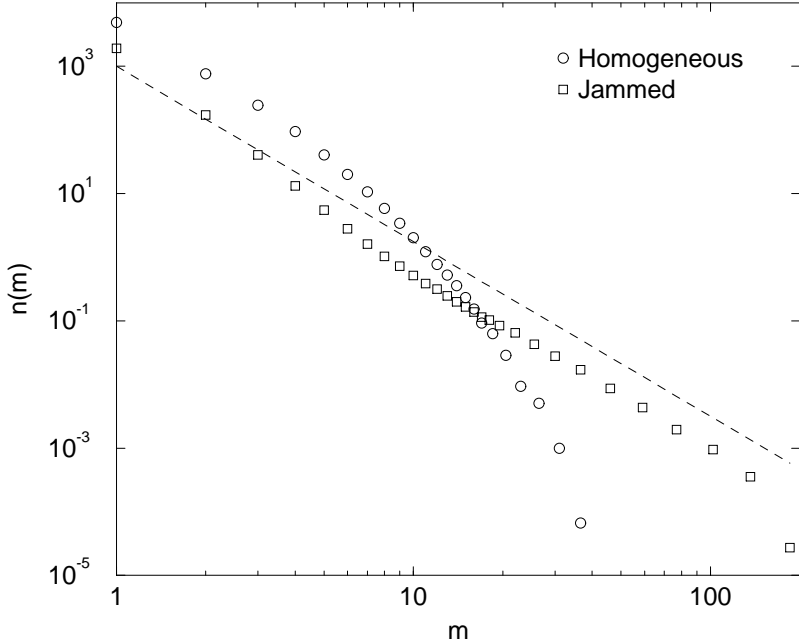


Fig. 6. Log-log plot of the steady state cluster size distribution for both unjammed and jammed systems with  $T = 0.006$ . The system size is  $900 \times 150$ ,  $c = 0.06$  and  $\dot{\gamma} = 6/1490 \simeq 0.004$ . The dashed line is proportional to  $m^{-2.75}$  and is shown to guide the eye.

exponent close to  $-2.75$ . However,  $n(m)$  decays faster than a power law for  $m$  greater than about 100. It is not clear whether this is a finite system-size effect or the true asymptotic behaviour. For jammed systems, the situation is further complicated by the fact that the cluster size distribution is spatially inhomogeneous (see figure 3).

We have found two different regimes of behaviour in the jammed state as  $T$  is varied. Figure 7 shows the variation of  $s_0$  with time in the (jammed) steady state with  $T = 0.007$  (the other parameters are the same as for figure 5). The average cluster size  $s_0$  appears to fluctuate about a value close to 3.25 for some time before increasing suddenly to more than 4.0; it then gradually falls back to about 3.25. We have found that this behaviour is due to splitting and reforming of the spanning cluster. We have already seen in figure 3 that a spanning cluster is narrowest at its centre. If  $T$  is sufficiently small, the spanning cluster does not split. However, when  $T$  is sufficiently large the spanning cluster may split in two, whereupon the two resulting clusters separate. At this point, the two large clusters grow by aggregating with smaller clusters before meeting again and reforming the spanning cluster (due to the periodic boundary in the flow direction). Upon reforming, the spanning cluster is larger (it contains more particles) than when it split; this is because the two large

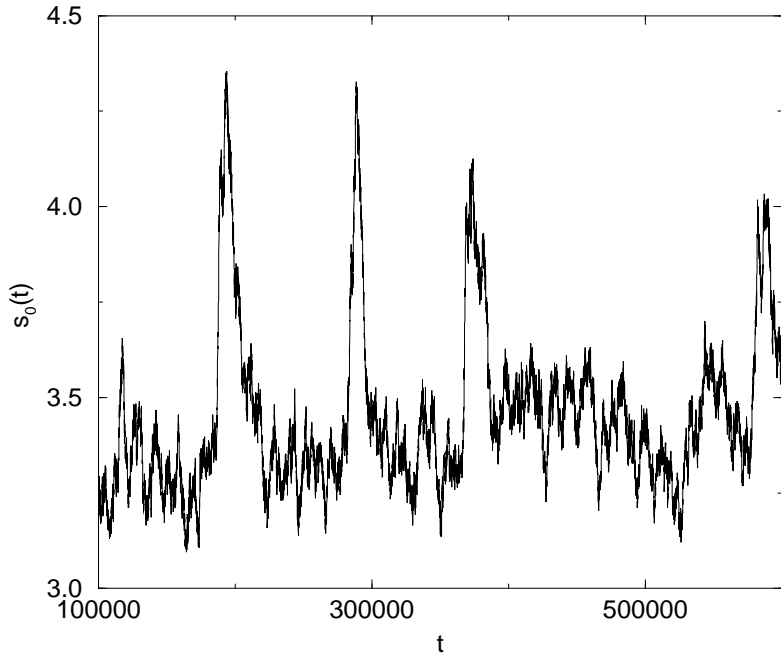


Fig. 7. Average cluster size  $s_0$  against time for a  $900 \times 150$  system with  $T = 0.007$ ,  $c = 0.06$  and  $\dot{\gamma} = 6/1490 \simeq 0.004$ .

clusters formed as a result of the split grow significantly before recombining. This explains the sudden rises in average cluster size seen in figure 7. The newly reformed spanning cluster gradually loses particles before splitting once more. The steady state is cyclic – a spanning cluster is stable only in the sense that once it splits, it always reforms. Close examination of figure 5 reveals a kink in the jammed branch of  $s_0(T)$  around  $T = 0.007$ . This is caused by the change in behaviour from a non-cyclic steady state to a cyclic one. If  $T$  is further increased beyond about 0.018, the two large clusters formed when a spanning cluster splits may become unstable and break up (due to fragmentation dominating shear-induced aggregation). An unjammed system then results and there is no longer a jammed steady state. It is not clear to what extent the splitting of spanning clusters is affected by system size.

### 3.2 Jamming Kinetics

The above concludes our discussion of the steady state properties of the model; we now consider the approach to the steady state when the system spontaneously jams from an initial condition of particles positioned at random. Figure 8 shows a snapshot of a system in the process of jamming 7000 time-steps after the particles were positioned at random. Clusters with a large range of

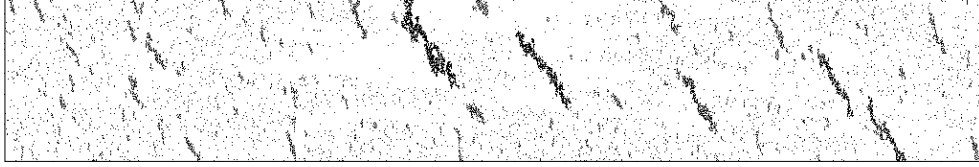


Fig. 8. Snapshot of a  $1200 \times 200$  system undergoing jamming at  $t = 7000$ . The particles were positioned at random at  $t = 0$ . The simulation parameters were  $c = 0.06$ ,  $T = 0.002$  and  $\dot{\gamma} = 8/1990 \simeq 0.004$ .

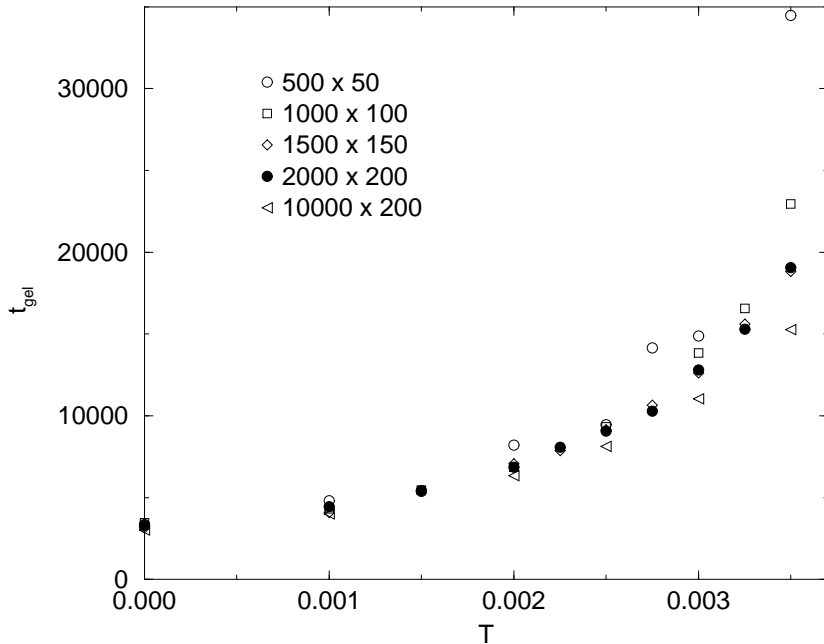


Fig. 9. Plot of  $t_{\text{gel}}$  against  $T$  for various system sizes. The simulations had  $c = 0.06$  and  $\dot{\gamma} = 8/1990 \simeq 0.004$ . The particles were positioned at random at  $t = 0$ . We averaged over between 10 and 20 independent runs.

sizes are visible.

We define the gel time  $t_{\text{gel}}$  as the time at which a spanning cluster first appears in the system. Santra and Herrmann [10] found (by extrapolation) that, for  $T = 0$ ,  $t_{\text{gel}}$  is finite for an infinite system. Figure 9 shows a plot of  $t_{\text{gel}}$  against  $T$  for different system sizes. It appears that as system size is increased for the fixed aspect ratio  $L/W = 10$ ,  $t_{\text{gel}}(T)$  converges. A fit to the data for the  $2000 \times 200$  system indicated that  $t_{\text{gel}}$  increases more quickly than  $\exp(T)$  and it is possible that it diverges for some finite value of  $T$ ; this is consistent with the presence of a phase transition at finite  $T$ . However, due to the large amount of computational effort required to obtain  $t_{\text{gel}}(T)$ , we have been unable to confirm this unambiguously. Also, figure 9 shows that  $t_{\text{gel}}$  depends on the aspect ratio of the system since  $t_{\text{gel}}$  for the  $10000 \times 200$  system is consistently

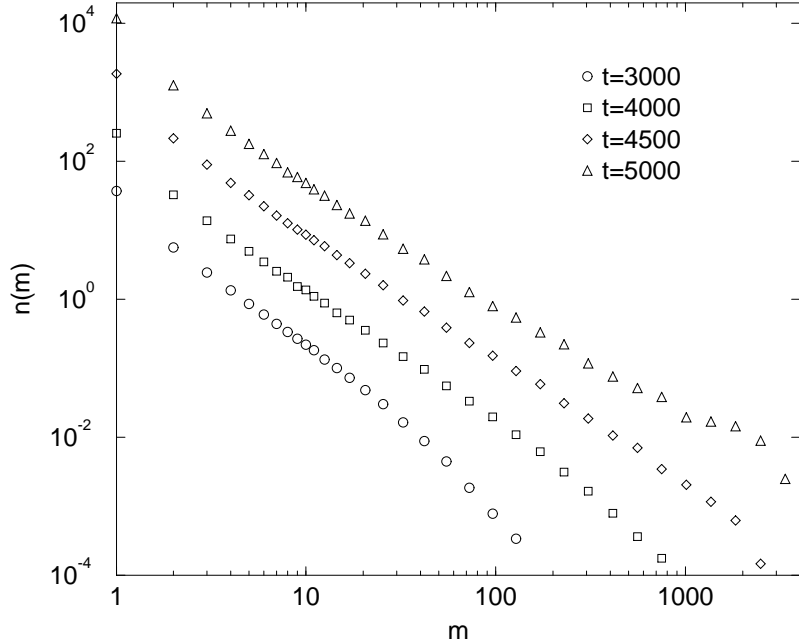


Fig. 10. Log-log plots of  $n(m)$  at different times for  $T = 0.001$ . The system size was  $10000 \times 200$  and  $c = 0.06$ ,  $\dot{\gamma} = 8/1990 \simeq 0.004$ . The particles were positioned at random at  $t = 0$ . We averaged over 12 independent runs. The data has been shifted vertically for clarity.

smaller than for the  $2000 \times 200$  system.

In a gelling system, we expect the pre-gelation cluster size distribution to have the scaling form [12,13]

$$n(m, t) \sim m^{-\tau} f\left(\frac{m}{s_1(t)}\right) \quad (7)$$

for large cluster sizes, with the typical cluster size  $s_1(t)$ , given by (6), diverging as  $t \rightarrow t_{\text{gel}}$ . Since the number of particles  $N$  is conserved, we must have  $\tau > 2$ . The above scaling *ansatz* is expected to apply for an infinite system. In our finite systems, we find evidence of such scaling for  $T \geq 0$  although finite-size effects are large.

Figure 10 shows a log-log plot of  $n(m)$  for  $T = 0.001$  at four different times (note that the curves have been shifted vertically for clarity). Power law behaviour appears gradually and is present over the largest range of cluster sizes at  $t^* \simeq 4500$ . We define  $t^*$  to be the time at which we see power law behaviour of  $n(m)$  over the maximum range of  $m$ . By  $t = 5000$ , spanning clusters have formed and a “bump” has begun to form in the tail of the distribution. By

fitting a power law to the  $n(m)$  for large  $m$  at  $t = t^*$ , we find the exponent  $\tau \simeq 1.9$ . Since for an infinite system  $\tau$  must be greater than 2, we conclude that finite-size effects are strong. Indeed, this is not surprising since we find, for  $T \leq 0.0025$ , that  $t^* \simeq t_{\text{gel}}$  (as expected in gelling systems) so that there are clusters with size of order the system size present at time  $t^*$ . However, for  $T = 0.003$  and  $T = 0.0035$  we find that  $t^*$  is somewhat smaller than  $t_{\text{gel}}$ , an anomaly which we are unable to explain but which may be due to finite-size effects.

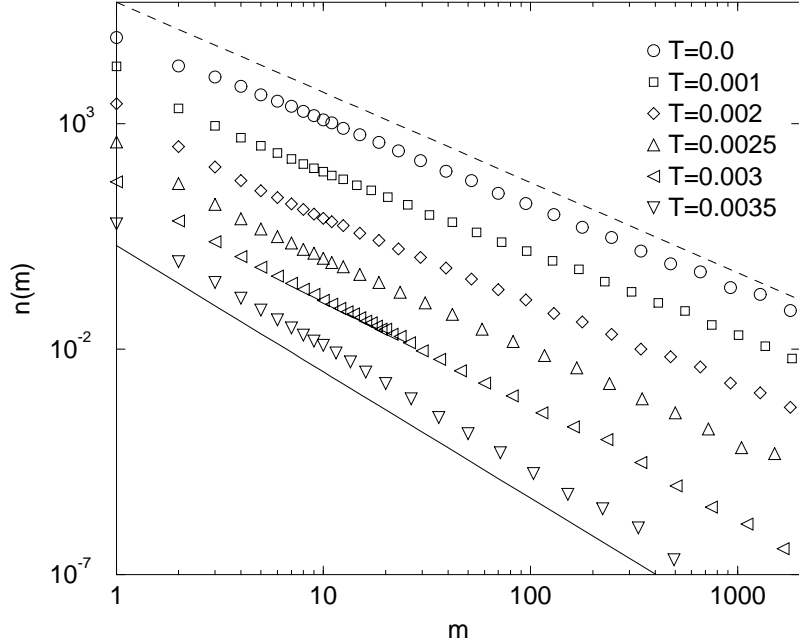


Fig. 11. Log-log plots of  $n(m)$  for various values of  $T$  after a time  $t^*(T)$ . The system size was  $10000 \times 200$  and  $c = 0.06$ ,  $\dot{\gamma} = 8/1990 \simeq 0.004$ . The values of  $t^*$  are 3400, 4500, 7000, 8500, 10000 and 12000 (in order of increasing  $T$ ). We averaged over 12 runs for each value of  $T$ . The data has been shifted vertically for clarity. The dashed line is proportional to  $m^{-2}$  and the solid line is proportional to  $m^{-2.8}$ ; they are shown to guide the eye.

Figure 11 shows log-log plots of  $n(m)$  at  $t^*$  for several values of  $T$ . A power law cluster size distribution (for  $m$  larger than about 10) is present for all values of  $T$ . The slopes of the power law regions decrease with increasing  $T$  (for  $T > 0$ ), suggesting that the exponent  $\tau$  varies significantly with  $T$  and hence that it may be non-universal. Further careful study of finite-size effects would be required to clarify this point.

## 4 Simulation Issues

The “counter” scheme [10] for performing cluster flow described in section 2 is not the only one that can be imagined. However, we have found that it has important advantages over other schemes.

For example, a simpler way of implementing cluster motion in the direction of flow is, at each time-step, to let each cluster move forward one site with probability  $v$ , where  $v$  is the velocity of the cluster. However, there are seemingly insurmountable difficulties with this stochastic implementation of cluster flow. To illustrate this point, let us consider how clusters aggregate and grow. Aggregation occurs when one cluster catches up with a slower neighbouring cluster. We wish the imposed shear to be the dominant factor in the aggregation. However, if clusters move forward stochastically, as in the scheme just described, fluctuations (in addition to the imposed velocity gradient) will cause clusters to aggregate. For example, a cluster with velocity  $v_1$  may move forward in several successive time-steps at the same time as a cluster with velocity  $v_2 > v_1$  does not move at all, possibly resulting in the spurious aggregation of the clusters. Indeed, we have found that when the stochastic implementation of cluster flow just described is used (instead of the counter scheme described in section 2), stochastic aggregation of clusters dominates aggregation due to the imposed shear for practical parameter values.

A further advantage of the counter dynamics for flow is that it is much closer to being Galilean invariant than a stochastic implementation of cluster flow. This is because, for stochastic flow, the size of the fluctuations in the motion of a cluster, and hence the rate of cluster-cluster aggregation, is strongly dependent on the absolute magnitude of the velocity  $v(y)$ . It is well-known that the variance of the displacement of an independent random walker hopping in one direction with probability per time-step  $v$  is proportional to  $v(1 - v)$ ; we therefore expect the rate of cluster-cluster aggregation for stochastic cluster flow to be greatest for  $v = 0.5$  and smallest for  $v = 0$  and  $v = 1$ . We have confirmed that this is indeed the case in simulations. This is a potentially serious problem in simulation of a shear flow since  $v$  varies across the width of the lattice.

Since the counter implementation of cluster flow is deterministic, the problems peculiar to stochastic cluster flow just discussed are circumvented. The counter scheme is, however, not without its limitations. Figure 12 shows the average cluster size of clusters whose centre of mass lies in lane  $y$  as a function of  $v(y)$  for two unjammed systems with different concentrations. The average cluster size is smallest for  $v = 0$  and  $v = 1$  due to the presence of the fixed walls. However, the cluster size grows quite slowly as one moves in from either wall and we have checked that the reason for this is that  $v$  is in the vicinity

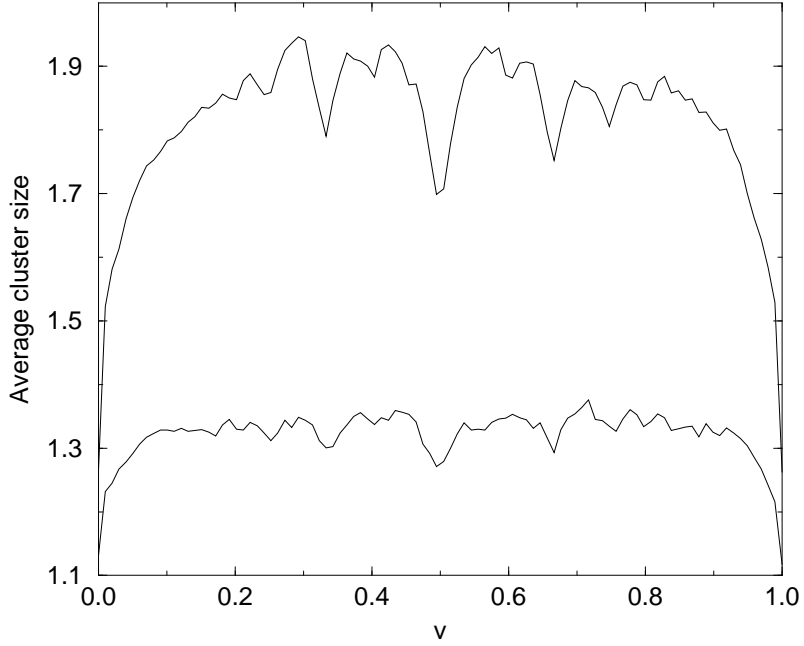


Fig. 12. Mean size of clusters having velocity  $v$  in two unjammed systems (averaged over  $10^5$  time-steps in the steady state). In both cases, the system size is  $400 \times 100$  with  $v_{\min} = 0$  and  $v_{\max} = 1$ . The top curve is for  $c = 0.15$  and  $T = 0.045$  while for the bottom curve,  $c = 0.07$  and  $T = 0.02$ .

of either 0 or 1. Similarly, a deep minimum in the average cluster size is evident around  $v = 1/2$ , with less pronounced minima also evident around  $v = 1/3, 2/3, 1/4, 3/4$ , etc. Clearly, the counter updating scheme has a systematic effect on the cluster-cluster aggregation rate, breaking Galilean invariance by introducing a velocity dependence of the cluster-cluster aggregation rate. Not surprisingly, the effect diminishes as  $c$  is decreased. In our simulations, we have attempted to minimise the effect of the spatial inhomogeneity caused by the updating scheme by working at low concentration and avoiding velocities less than 0.1 or greater than 0.9. For the concentration values we have used ( $c \leq 0.07$ ), it is clear that the shear is the dominant factor driving cluster-cluster aggregation since the average cluster size varies significantly with shear rate (see figure 4).

It is clear that lattice models are not ideally suited to the simulation of a Galilean invariant phenomenon such as shear-induced aggregation, although they are a relatively simple and efficient approach to the problem. However, there are physical situations where Galilean invariance is not respected, an example being (multi-lane) traffic flow where the concept of being “at rest” is absolutely defined. Indeed, lattice models of multi-lane traffic flow have recently been studied [14]. The present model could be interpreted as a mul-

tilane flow in which vehicles cannot pass one another without an empty lane being present between them as they do so. However, the rules adopted for determining cluster velocities would themselves then have to be chosen non-Galilean-invariant (a cluster would travel only as fast as its slowest member). Apart from rotation effects [11], the presence or absence of Galilean invariance is (arguably) the major difference between colloidal and vehicular jamming.

In summary, the counter scheme [10] is a deterministic way of implementing cluster flow which circumvents some of the difficulties associated with a stochastic implementation of cluster flow. In addition, it only allows single step movements of clusters and thus avoids potential problems associated with collisions of clusters and double occupancy of sites.

## 5 Discussion

In this work we have studied a simple stochastic model of shear-induced clustering on a  $2d$  lattice. Our results strongly suggest that a discontinuous transition occurs, with strong hysteresis, from an unjammed state to a jammed state as the shear rate is increased or temperature decreased. As the system jams, the distribution of clusters becomes power law. However, the exponent may have a non-trivial temperature dependence, appearing to vary continuously.

Our conclusions are based on the study of finite systems and, while we have presented strong evidence in favour of the presence of a discontinuous phase transition in the model, care is required in identifying such a phase transition [7]. It would be useful therefore to study systematically finite-size effects in the system, as well as the effect of varying the aspect ratio. Also, we have not considered rotation of clusters but it should be possible to do so following ref. [11].

It is interesting to compare the present transition to several other models of reversible cluster-cluster aggregation in which the aggregation is due to diffusion of clusters, rather than an imposed shear. In the conserved-mass aggregation model of Krishnamurthy *et al* [15] a transition from a disordered (unjammed) phase to a phase containing an infinite cluster occurs as the rate of single particle dissociation increases. The infinite aggregate phase exhibits a power law cluster size distribution. However, in contrast to the present model, the transition in that work is reminiscent of Bose condensation and does not exhibit hysteresis. We also mention the work of Shih *et al* [16] and Haw *et al* [17] where diffusion limited cluster-cluster aggregation with finite bond energy (thus allowing fragmentation) is studied in the context of colloidal gels.

## Acknowledgements

OJO is supported by a University of Edinburgh Postgraduate Research Studentship and gratefully acknowledges the award of a Royal Society Summer Studentship during the initial part of this work. MRE is a Royal Society University Research Fellow.

## References

- [1] see e.g., W.J. Frith, P. D'Haene, R. Buscall and J. Mewis, *J. Rheol.* 40 (1996) 531; J. Bender and N.J. Wagner, *J. Rheol.* 40 (1996) 899.
- [2] I. Wunderlich, H. Hoffmann and H. Rehage, *Rheol. Acta* 26 (1987) 532; R. Bruinsma, W.M. Gelbart and A. Ben-Shaul, *J. Chem. Phys.* 96 (1992) 7710; P. Boltenhagen, Y. Hu, E.F. Mattheys and D.J. Pine, *Phys. Rev. Lett.* 79 (1997) 2359.
- [3] J.F. Brady and G. Bossis, *Annu. Rev. Fluid Mech.* 20 (1988) 111.
- [4] R.S. Farr, J.R. Melrose and R.C. Ball, *Phys. Rev. E* 55 (1997) 7203.
- [5] Statistical Mechanics of Driven Diffusive Systems, eds. B. Schmittmann and R.K.P. Zia (Academic Press, UK, 1995).
- [6] For a review, see J. Krug, to appear in: *Traffic and Granular Flow '97*, (Springer, Singapore, 1998).
- [7] O.J. O'Loan, M.R. Evans and M.E. Cates, *preprint cond-mat/9712112*.
- [8] O.Biham, A.A. Middleton and D. Levine, *Phys. Rev. A* 46 (1992) 6124.
- [9] B. Schmittmann, K. Hwang and R.K.P. Zia, *Europhys. Lett.* 19 (1992) 19.
- [10] S.B. Santra and H.J. Herrmann, *Physica A* 218 (1995) 298.
- [11] T. Kovács and G. Bárdos, *Physica A* 234 (1997) 665.
- [12] P.G.J. van Dongen and M.H. Ernst, *J. Stat. Phys.* 50 (1988) 295.
- [13] P.G.J. van Dongen and M.H. Ernst, *Phys. Rev. Lett.* 54 (1985) 1396.
- [14] see e.g., P. Wagner, K. Nagel and D.E. Wolf, *Physica A* 234 (1997) 687.
- [15] S. Krishnamurthy, S.N. Majumdar and M. Barma, *preprint cond-mat/9709117*.
- [16] W.Y. Shih, J. Liu, W.H. Shih and I.A. Aksay, *J. Stat. Phys.* 62 (1991) 961.
- [17] M.D. Haw, M. Sievwright, W.C.K. Poon and P.N. Pusey, *Adv. Colloid Interface Sci.* 62 (1995) 1.